Effects of waves on BEM theory in a marine tidal turbine environment

Jeremiah Fulton, Luksa Luznik, Karen Flack, Ethan Lust
Mechanical Engineering Department,
U.S. Naval Academy
Annapolis, MD, USA
luznik@usna.edu

Abstract—**Blade Element Momentum (BEM) theory is a well understood and proven method for modeling blade loads and determining steady state performance characteristics of wind turbines. Recently this theory has successfully been applied to horizontal axis marine current turbines when incorporating modifications that lead to better predictions of turbine performance for a range of operating conditions. Relatively little work exists in the implementation of BEM theory in a marine environment with surface gravity waves. A better understanding of the effects of waves on tidal turbines is necessary to predict fatigue loading that can eventually lead to blade failure. This paper presents a BEM numerical model that incorporates the unsteady velocities due to the presence of waves and assesses the effects of waves on tidal turbine performance. Numerical results of the coefficient of power (C_P) and coefficient of thrust (C_T) match closely with experimental results for the mean C_p and C_T for a range of tip speed ratios. The model is also able to predict the instantaneous amplitudes of the performance characteristics as compared with the measured values except for the BEM calculated thrust which shows a 20% reduction in amplitude.**

Keywords—marine current turbine; BEM theory; waves

I. Introduction

The Blade Element Momentum (BEM) method uses a combination of momentum theory and blade element theory. Momentum theory uses a control volume analysis of the forces at the blade based on conservation of linear and angular momentum. Blade element theory considers the forces on a section of the blade based on blade geometry. The combination of these two methods leads to what is known as strip theory or blade element momentum theory. This theory can be used to relate geometrical blade data and flow conditions to power output and other parameters such as thrust and torque loading of the blades [1]. BEM theory is a well understood and proven method for modeling blade loads and determining steady state performance characteristics of wind turbines. Recently the BEM model has been implemented for horizontal axis marine current turbines and [2] discusses in detail the challenges and modifications needed to better predict the performance of a marine rotor under a range of operating conditions. However, relatively little research exists in the implementation of BEM theory in a marine environment with waves. Tidal turbines are becoming increasingly popular as clean alternative for producing power. In almost every marine environment where a tidal turbine could be situated, there are also waves. The effect of waves on tidal turbines is essential for two primary reasons. First, unsteady flow causes fatiguing of the turbine blades which could lead to eventual failure. Second, unsteady flow causes variations on coefficients of power which causes instabilities in power outputs.

The objectives of this paper are to document modifications made to an existing in-house BEM code and to compare results from the computational model to experimental results obtained from testing a two bladed horizontal axis model turbine in a tow tank facility.

II. Methods

A. USNA BEM Model

Blade Element Momentum theory [1] was implemented into the numerical model as described in Walker et al. [3]. Specific inputs to this model include experimentally obtained lift and drag coefficients for a NACA 63-618 airfoil section. This particular airfoil was selected for a 1/25 scale (D=0.8m) two bladed horizontal axis turbine model (Fig. 1) that was extensively tested at the USNA Hydrodynamic laboratory. The numerical model includes a tip factor correction coefficient in order to correct for three-dimensional flow, and a coefficient of lift correction to account for stall effects as described by Snel et al. [4].

The addition of waves to the BEM model requires several considerations. First, the axial flow component will vary in space and time due to presence of unsteady wave motions. Second, the tangential flow over the rotating turbine blades will be affected by vertical wave velocity components. Third, inertia must be considered due to the accelerating/decelerating nature of the turbine rotational speed as the wave passes over the turbine. Implementation of each of these modifications into the numerical model is discussed in the following sections.

B. Kinematics Modifications of the BEM Model

In the steady flow case, there are two components of fluid velocity that, when combined with lift and drag coefficients, can be used to determine the induction factors and ultimately

This study was sponsored by the Office of Naval Research

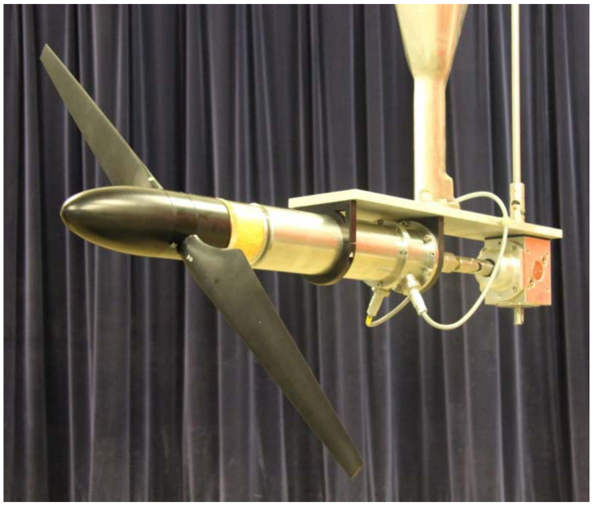

Figure 1: 1/25 scale model of two bladed horizontal axis turbine. Diameter D=0.8m. Blades have NACA 63-618 airfoil section.

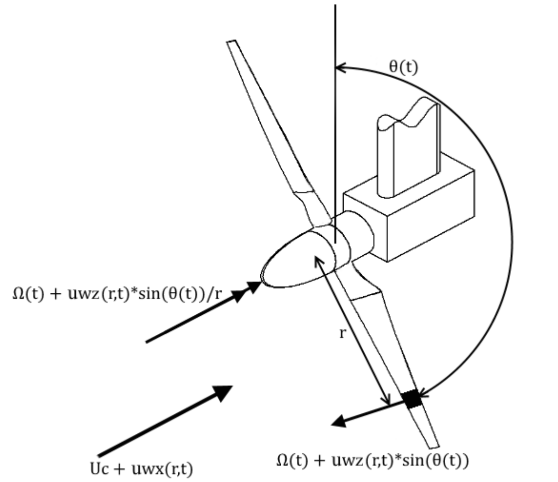

Figure 2: Isometric sketch of kinematics seen by the turbine blades with waves. Blade is rotating clockwise, θ is turbine position referenced to the vertical.

the power $C_P = \frac{Q\Omega}{\frac{1}{2}\rho U_c^3 \pi R^2}$ and thrust $C_T = \frac{T}{\frac{1}{2}\rho U_c^2 \pi R^2}$ coefficients of the turbine. Here Q is the turbine torque, ρ is the fluid density, T is the developed thrust, R is the blade radius. U_c is the inflow velocity (current speed) that travels axially past the turbine. The second is a tangential velocity (**Ω**), albeit relative, that is produced by the rotational motion of the turbine. The addition of waves changes the two components of the fluid flow. As a result, inflow velocity experienced by the turbine rotor becomes a function of time and depth and contains linearly superimposed contributions of the steady current velocity (i.e. carriage speed) and the fluctuating axial wave velocities. Furthermore, turbine rotational speed is altered by the vertical component of the wave field, resulting in fluctuating turbine rotational speed. Equations (1) and (2) show the implementation of the wave velocities in the modified BEM code.

$$U_{rel}(r,t) \equiv U_c + u_{wx}(r,t) \tag{1}$$

$$\Omega_{rel}(r,t) \equiv \Omega(t) + \frac{u_{wz}(r,t)}{r}\sin(\theta(t)) \tag{2}$$

Where u_{wx} and u_{wz} are the axial and vertical wave induced velocities, respectively using the second order Stokes solution for wave velocities [5]. Index *r* represents the radius of a blade element, and *θ(t)* is the instantaneous position of the turbine defined from the vertical, as shown in Fig 2.

Experimental results by our group [6] show that waves produce a variation in the amplitude of the rotor rotational speed *Ω(t)*. Difficulty arises in knowing exactly how rotational speed amplitude varies with incident waves and how to implement this feature in the BEM model. In the steady case, the rotational speed in the BEM model is calculated using a specified tip speed ratio ($TSR = \frac{R\Omega}{U_c}$), however in the case with waves, a mean TSR is specified, but its variations with waves cannot be determined in the same manner. In order to work around this issue, a non-dimensional experimental relationship was developed between the wave steepness defined as $\frac{H}{L_w}$ where H is wave height and L_w is the wavelength, and the product of wave period, T_w and the rotational amplitude of the turbine Ω_A. This relationship is shown in Figure 3 where the experimental data are from tow tank experiments [6] using the present model turbine. The experimental characteristics of the regular waves from that experiment are given in Table 1.

TABLE 1: Wave Characteristics [6]

Wave length (m)	**Steepness**	**Description**	**Wave Period (s)**	**Energy (J/m)**
15.7	0.005	Shallow	3.2	104
8.8	0.011	Intermediate	2.4	104
3.9	0.038	Deep	1.6	104
8.25	0.022	Intermediate	2.3	339

The experimental data span two regular waves with variable steepness and constant wave energy. The energy per unit width of the wave is defined as $E = \frac{1}{8}\rho g H^2 L_w$ where g is gravitational constant. The downward slope shown in Fig 3 demonstrates that as the wave gets steeper its period decreases. A decreased period means that the turbine has less time to respond to the changing wave flow profile and consequently has less variability. Since both wave period and rotational amplitude decrease as steepness increases, their product also decreases with increasing slope. The two data points that fall above the uncertainty bounds are likely due to a slight change in the turbine pitch between data sets. Scatter of the data at each wave steepness is attributed to the variability with mean TSR, which for this data sets span from 6.8 to 8.5 (see also Fig 5).

From the established linear relationship between steepness and $\Omega_A T_w$ for any given wave steepness and period with a wave energy in range of 104-339 J/m, the corresponding rotational amplitude Ω_A can be determined. Using the rotational amplitude and mean rotational speed Ω_m from the chosen mean TSR, the turbine instantaneous rotation

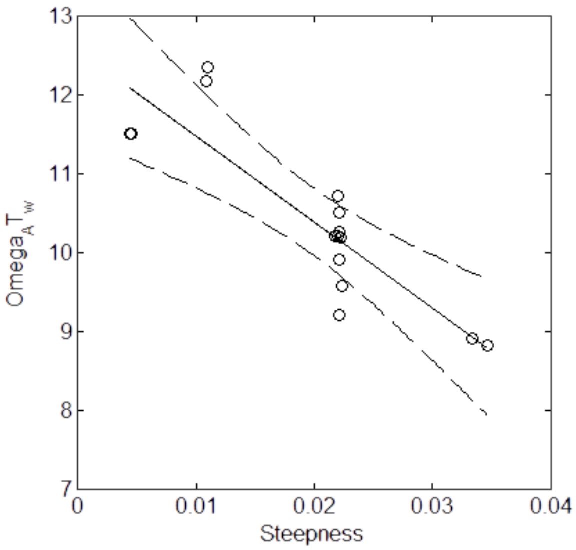

Figure 3: Relationship between steepness $\frac{H}{L_w}$ and non-dimensional term $\Omega_A T_w$. Data shown are for two waves with energies of 104 J/m to 339 J/m. Regression line is shown (full line) together with upper and lower dashed lines indicating upper and lower 99% confidence bounds.

speed can be calculated as:

$$\Omega(t) = \Omega_A \cos(kx - \sigma t) + \Omega_m \qquad (3)$$

Here we assume cosine function response behavior of the rotational amplitude based on the cosine function "forcing" of the incoming waves. The turbine instantaneous displacement can in turn be calculated as:

$$\theta(t) = -\frac{\Omega_A}{\sigma}\sin(kx - \sigma t) + \Omega_m t \qquad (4)$$

Finally, the relative instantaneous axial and tangential flow velocities are then used to find the radial distribution of local tip speed ratio, λ_r as:

$$\lambda_r(r,t) = \frac{\Omega(t)\, r + u_{wz}(\mathrm{r,t}) \sin(\theta)}{U_c + u_{wx}(r,t)} \qquad (5)$$

The resulting local tip speed ratios are used as inputs and the BEM model is run for each time-step as if the system is at steady state. This, however, neglects any form of transient response that is seen in the turbine due to its own inertia. To correct for this, turbine inertia is considered next.

C. Inertia Modifications of the BEM Model

Due to the accelerating/decelerating nature of the turbine in the wave field, inertia must be considered. In this paper we only consider the turbine rotational mass moment of inertia. The calculation of inertia was done using two methods. In the first method the inertia is calculated theoretically by modeling the blades as thin rods and the hub as a solid cylinder [7] resulting in I_{theory}=0.096 kg-m^2. The second empirical method combines BEM simulations with measurements of thrust, torque and rpm obtained during experiments [6] for the present model turbine in the presence of waves. The mass moment of inertia is estimated using equation:

$$I = \overline{\frac{Q_{BEM}(t) - Q_{dyno}(t)}{\dot{\Omega}}} \qquad (6)$$

where Q_{BEM} is the BEM calculated torque for a specific experimental run with waves, Q_{dyno} is the measured torque and $\dot{\Omega}$ is the turbine's rotational acceleration obtained from the turbine measured rpm record. The overbar indicates a time average over the length of the run covering approximately 20 wave cycles. The resulting value of empirically determined rotational mass moment of inertia is $I_{empirical}$=0.087 kg-m^2. Both estimated values are close, and the theoretical value helps to validate the empirical estimate. Due to simplified geometries used the theoretical solution compared to the actual relatively complex blade geometry for the turbine model, the empirical value of inertial was used in all subsequent BEM simulations.

III. Results

A. Steady State Validation

As a part of the validation process the modified BEM code was run at steady state. Figure 4 shows calculated power and thrust coefficient as a function of TSR compared to the steady state BEM predictions published in [3]. Results from the modified BEM method fall on top of steady state results thus confirming that present modifications to the BEM model do not alter the steady state results.

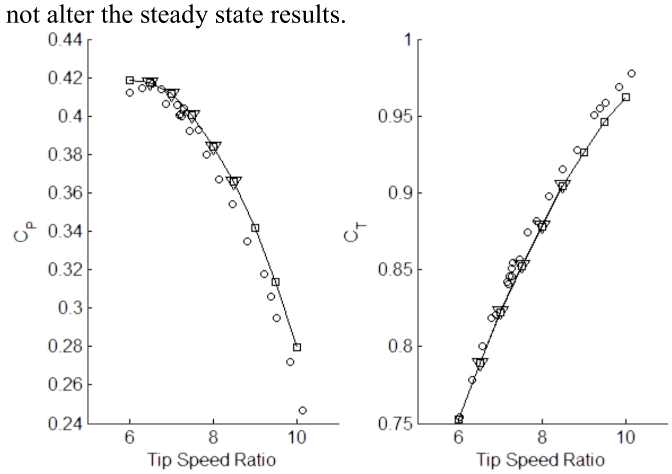

Figure 4: Steady state BEM method validation. Squares show BEM simulations for steady state conditions (quiescent flow) from [3] and upside-down triangles results from modified BEM method described in this paper. Circles are experimental data for steady state flow conditions [3].

B. Average Performance Characteristis in presence of waves

Figure 5 shows average performance characteristics calculated using the modified BEM model together with the baseline C_P and C_T data of the model turbine in quiescent flow and with the presence of surface gravity waves. Experimental power and thrust coefficients for cases with waves have been corrected for Stokes drift [6]. The experimental data matches with the BEM model results over a range of tip speed ratios (TSR), although a consistent computational under prediction is noted. It should also be noted that experimental results suggest that average power and thrust coefficient are not dependent on the wave form, as data with waves with different energies are

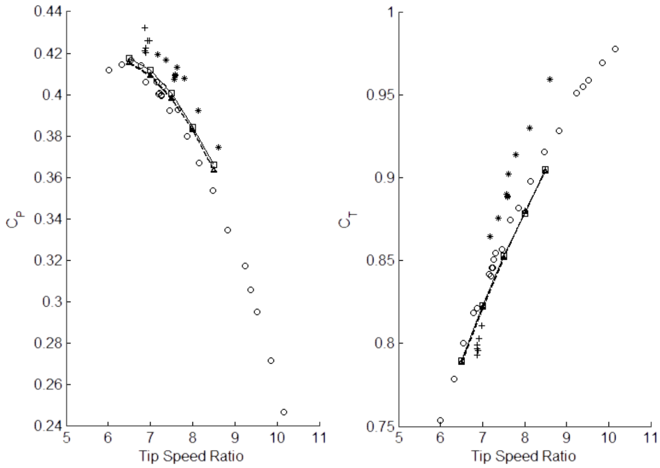

Figure 5: Cp and Ct data as a function of mean tip speed ratio TSR. Solid/dashed lines are BEM simulations for waves with 339 J/m and 104 J/m energy and 0.022 and 0.005 steepness. Crosses and stars are Cp and Ct from measurements [6]. Circles are experimental steady state data.

within experimental scatter. The same trend is observed with the BEM simulations.

C. Instantaneous Response in the Presence of Waves

In order to assess the performance of the modified BEM model in terms of variability of turbine loading over a wave cycle, Fig 6 shows a time history of measured turbine thrust, torque, shaft rpm, free surface elevation (η) and corresponding calculated C_P and C_T over four wave cycles at an average TSR = 7.2. The wave characteristics for this particular data set are: wavelength L_w=8.3m, wave period T_w=2.3 seconds, and steepness=0.022. The BEM simulation for the same input wave and average TSR are shown in Fig 7.

All predicted amplitudes are comparable with the measured values except for the BEM calculated thrust which shows a 20% reduction in amplitude. Overall the mean C_P and

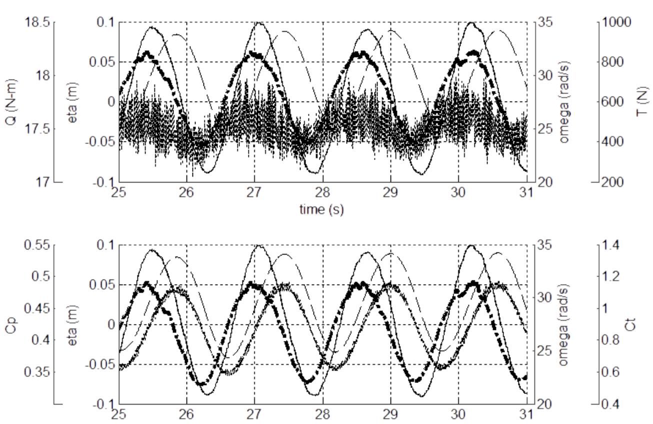

Figure 6: Time history of measured quantities. Top: Solid thin line is measured free surface elevation (η). Dashed thin line is rotational speed Ω. Heavy dash-dot line is thrust and noisy dotted line is torque. Bottom: Solid thin line is η. Dashed thin line is Ω. Heavy dash-dot line is Ct. Dotted thin line is Cp. TSR = 7.19

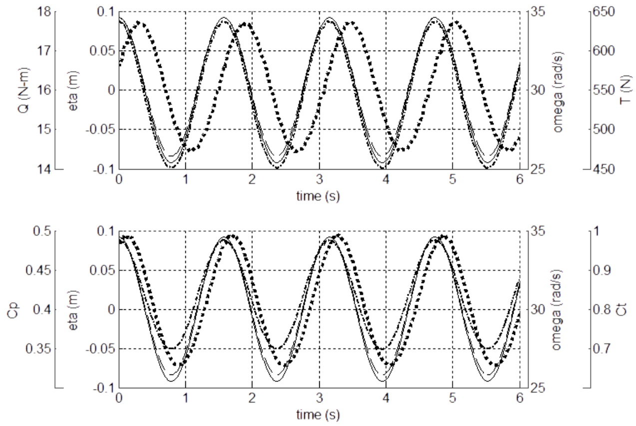

Figure 7: Time history of BEM results. Top: Solid line is η. Dashed line is Ω. Dash-dot line is thrust. Dotted thick line is torque. Bottom: Solid line is η. Dashed line is Ω. Dash-dot line is Ct. Dotted thick line is Cp. TSR = 7.19.

C_T, averaged over four cycles, is consistent with the mean results shown in Figure 5. However there are differences in phases between experimental and numerical results. As shown in Figure 6, the time history of measured thrust and corresponding thrust coefficient closely follow the time history of the free surface elevation. This suggests that any phase delay between the forcing wave field and the thrust developed by the turbine is small. This is consistent with the results of Maniaci and Li [8] who showed that the addition of axial added mass into the BEM calculations did not play a significant role. Since the present BEM model does not account for the axial added mass, the calculated thrust and C_T (Figure 7) are in phase with the free surface elevation.

The measured rotational speed of the turbine lags the free surface elevation due to initial transient. This is not accounted for in our BEM model thus the calculated time history of the rotational speed and the free surface are shown to be in phase. However, by accounting for the rotational mass moment of inertia in our BEM model, the calculated torque and C_P lag by approximately 10% of the encounter wave period and the free surface elevation record. Distinguishing the phase lag between the measured torque and free surface elevation is not possible due to the noisy torque signal. The experimental C_P lags about 20% the encounter period and the measured free surface elevation.

IV. Conclusions

The framework for an unsteady BEM code that incorporates surface gravity waves has been developed. This numerical model includes modifications to the kinematics of the fluid flow and includes a second-order Stokes wave field. Furthermore, the variability of the turbine rotational speed to different wave fields is incorporated in the model via an experimental/empirical relationship that allows for the calculation of a time dependent local tip speed ratio. Validations of the modified BEM model show that integrated time domain BEM predictions for power and thrust coefficients are consistent with the experimental results. Two further important results stem from this study:

1) The average power and thrust coefficient are not dependent on the wave form as data with waves with different energies follow the same trend within experimental scatter. A similar trend is observed with the BEM simulations.

2) Results experimentally confirm the Maniaci and Li [8] assertion that axial added mass does not play a significant role, and as a result, need not to be included in the BEM model. This is manifested by both the thrust and thrust coefficient closely following the time dependent free surface elevation record.

ACKNOWLEDGMENT

The authors thank Mr. John Zseleczky, Mr. Daniel Rhodes, Mr. Bill Beaver and the entire staff of US Naval Academy Hydromechanics Laboratory for their contributions in designing, building and testing of the model tidal turbine.

REFERENCES

[1] Manwell J., Mcgowan J. and Rogers A. Wind Energy Explained, Theory, Design and Application. West Sussex, United Kingdom. 2012. pp 91-155

[2] Masters I.,CMath, Chapman, J.C.,Willis, M.R.,Orme, J.A.C., “A robust blade element momentum theory model for tidal stream turbines including tip and hub loss corrections”, Journal of Marine Engineering & Technology, 10:1, 25-35 2011

[3] Walker, J.M., Flack, K.A., Lust, E.E., Schultz, M.P., Luznik, L., "The Effects of Blade Roughness and Fouling on Marine Current Turbine Performance", in 10th European Wave and Tidal Energy Conference 2013: Aalborg, Denmark.

[4] Snel H. et al,. "Sectional Prediction of Three-Dimensional Effects for Stalled Flow on Rotating Blades and Comparison with Measurements", 1993 Procedings of the EWEC Conference.

[5] Dean R., Dalrymple R. Water Wave Mechanics for Engineers and Scientists, Advanced Series on Ocean Engineering – Volume 2. Singapore. 1994. pp 58-59, 79-80, 305

[6] Lust, E.E., Luznik, L., Flack, K.A., Walker, J.M., Van Benthem, M.C., "The influence of surface gravity waves on marine current turbine performance", International Journal of Marine Energy. 2013. Pp 32-37

[7] Hibbeler R.C. Engineering Mechanics: Dynamics, Twelfth Edition, 2010.

[8] Maniaci, D.C., Li, Y., "Investigating the Influence of the Added Mass Effect to Marine Hydrokinetic Horizontal-Axis Turbines Using a General Dynamic Wake Wind Turbine Code", in OCEANS Conference 2011.